Electronic Supplementary Information on

Spherical α-$Ni(OH)_2$ Nanoarchitecture Grown on Graphene as Advanced Electrochemical Pseudocapacitor Materials

Shubin Yang, Xilin Wu, Changlun Chen, Huangli Dong, Wenping Hu, Xiangke Wang

Experimental details

S1. Synthesis of GN composites

GN composites composites were synthesized by controlling the mass ratio of graphene oxide (GO) and $Ni(OH)_2$ (shown in Scheme S1a). With the mass ratio of GO to $Ni(OH)_2$ varied at 1:1, 1:5, 1:10, 1:20, 1:30, 1:40, the resulting composites were denoted as GN1, GN 5, GN10, GN20, GN30, and GN40, respectively. For GN30, the typical experiment was as follows. GO was made via a modified Hummers method as previously reported.[1] In a typical reaction, 5 mg of GO powder was dispersed in 20 mL water under ultrasonication, with 470.55 mg of $Ni(NO_3)_2 \cdot 6H_2O$ then completely dissolved. Next, 283.5 mg hexamethylenetetramine (HMT, $C_6H_{12}N_4$) was quickly added and stirred together until the solution became homogeneous. The suspension was then sealed in 50 mL Teflon lined stainless steel autoclaves for hydrothermal reaction at 140 ºC for 10 hours. The final product was collected by centrifuge, washed several times with distilled water and ethanol, and finally dried in a vacuum oven at room temperature. Pure α-$Ni(OH)_2$ was also obtained by the aforementioned procedure for comparison.

S2. Sample Characterization

The crystal structures were analyzed by X-ray powder diffraction (XRD, X'Pert PRO) equipped with Cu Kα radiation (λ=0.15406 nm). Fourier Transforms Infrared spectroscopy (FT-IR) was carried out on a Bruker

EQUINOX55 spectrometer (Nexus) in KBr pellet at room temperature. X-ray photoelectron spectroscopy (XPS) spectrum was recorded with a Thermo VG Scientific Sigma Probe spectrometer. Transmission electron microscopy (TEM) images was taken on a TECNAI F20 (Philips) at 200kV. An energy-dispersive X-ray spectroscopy (EDS) instrument was attached to the JEOL 2010. The surface area of the synthesized materials was studied using BELSORP MINI II.

S3. Electrochemical Measurement

The electrochemical response was measured with a CHI660a analyzer with an interpersonal computer in an electrochemical cell, which contains the three electrode system. Ag/AgCl electrode filled with 3 M KCl was used as reference electrode, a platinum wire was used as counter electrode, and GN composites on nickel foam was used as a working electrode with 6 M KOH solution as the electrolyte. Electrochemical studies were carried out by measurement of cyclic voltammetry (CV) and impedance of half cells using AUTOLAB (ECO CHEMIE, PGSTAT 100). The working electrode was prepared as follows: ~1 mg of material was first mixed with polytetrafluoroethylene (from 60 wt.% water suspension, Aldrich) in a ratio of 100:1 by weight, and then dispersed in ethanol; the suspension was drop-dried into a 1 cm × 1 cm Ni foam (2 mm thick) for 1 h at 80 ºC; the foam with sample loaded was compressed before measurement. The supercapacitor devices are fabricated in the same way as in industry as shown in Scheme 1b. Electrochemical impedance spectroscopy (EIS) measurements were conducted for the working electrode in a frequency range of 100 kHz-0.01Hz with ac perturbation of 5 mV. The EIS data were analyzed using Nyquist plots, which represent the imaginary part (Z') and real part (Z'') of impedance. All tests were performed at room temperature. The specific capacitance was calculated by integrating the area under the CV curve to obtain the charge (Q) and then dividing by the mass of active material (m), the scan rate (v), the oxidation or reduction current (I), time differential (dt), and the potential window which indicates the voltage range of one sweep segment (ΔV) according to the following

equation: $C = \frac{\int Idt}{m\Delta V}$. Specific capacitance could also be calculated from the galvanostatic charge and discharge curves, using the following equation: $C = (I\Delta t)/(m\Delta V)$, where I is charge or discharge current, Δt is the time for a full charge or discharge, m indicates the mass of the active material, and ΔV represents the voltage change after a full charge of discharge.

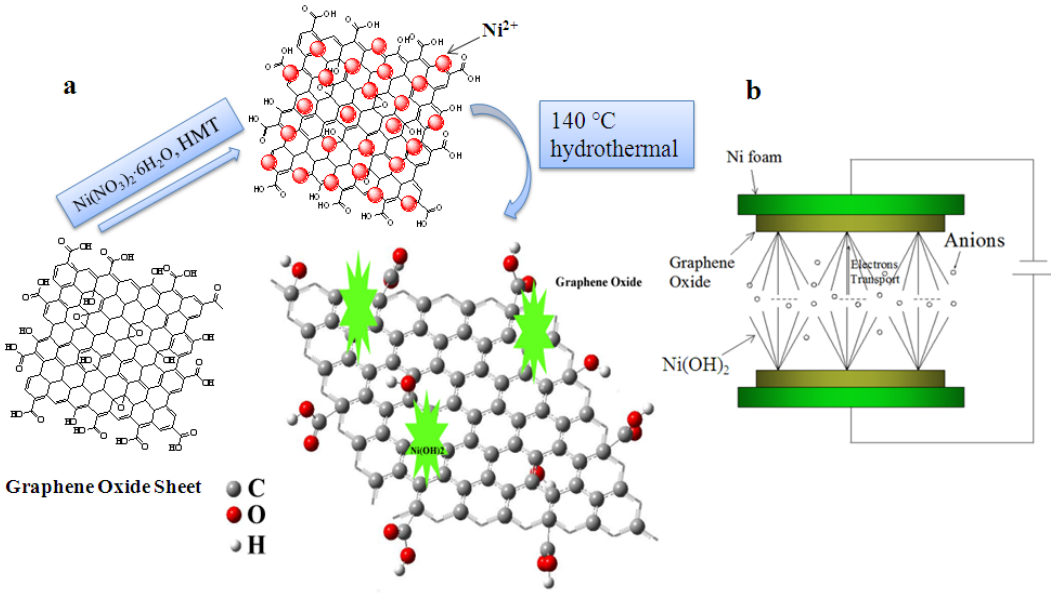

Scheme S1. Schematic illustration of the formation of graphene/α-$Ni(OH)_2$ nanocomposites (a) and the diagram of graphene/α-$Ni(OH)_2$ supercapacitor device (b).

S4. Characterization Results

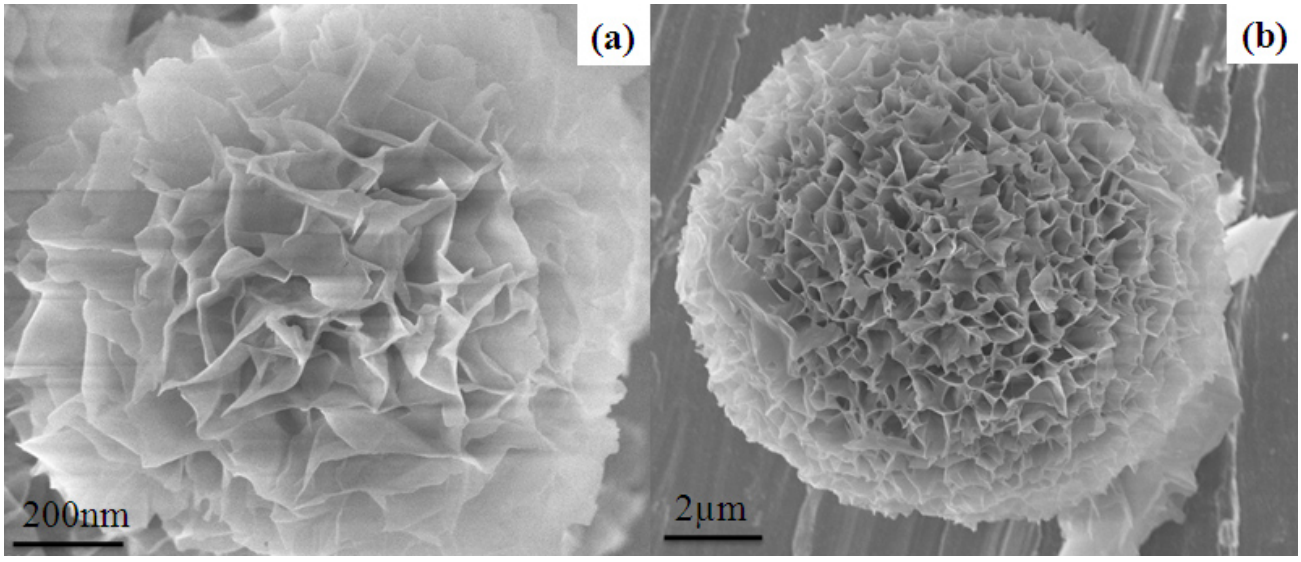

Fig. S1. SEM images of α-$Ni(OH)_2$ spheres (a), and GN20(b).

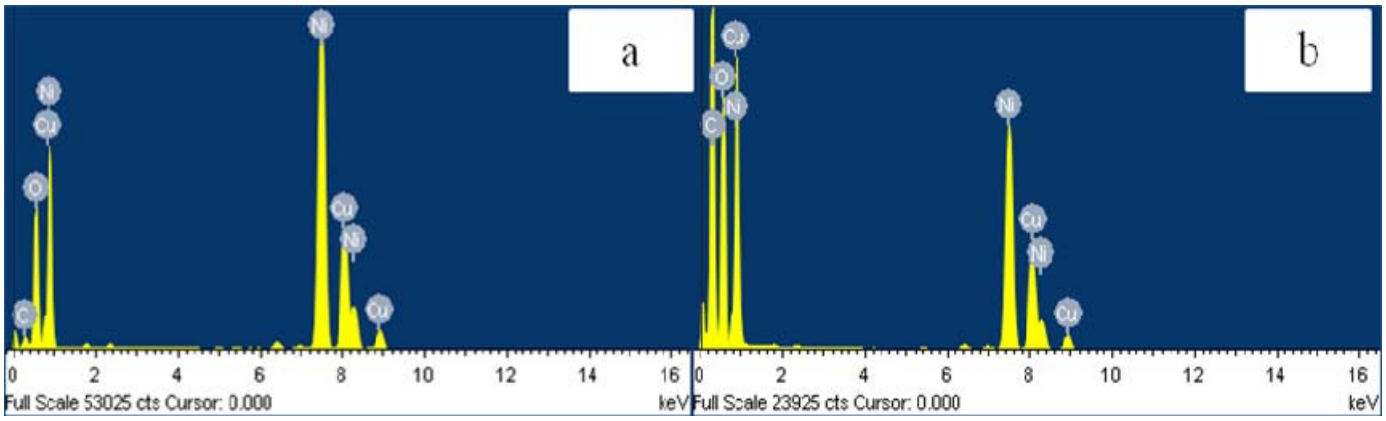

Fig. S2. EDS spectrum of GN20 (a), and GN5 (b). Cu peak came from the TEM grid.

Important information about the chemical compositions of GN composite can be further provided by XPS (Fig.S3). The photoelectron lines at binding energies of about 66, 111, 285, 531, 643, 714, 781, 855, 872, 977 and 1015 eV are attributed to Ni 3p, Ni 3s, C 1s, O 1s, Ni LMM, Ni LMM1, Ni LMM2, Ni $2p_{3/2}$, Ni $2p_{1/2}$, O KLL and Ni 2s, respectively. For GN20, the survey spectrum (Fig.S3a) shows mainly carbon (C1s) and oxygen (O1s) species. Detailed analysis of the C1s region is shown in Fig.S3b. The region of the C1s spectra can be deconvoluted into four functional groups:[2] (1) the non-oxygenated C (284.8 eV); (2) the carbon in C-O (286.5 eV); (3) the carbonyl carbon (C=O, 288.3 eV); and (4) the carboxylate carbon (O-C=O, 290.0 eV). In the Ni 2p region (Fig.S3c), the spectrum shows a number of extra lines marked as satellites in addition to the expected Ni 2p1/2 and Ni 2p3/2 signals (Ni $2p_{3/2}$: 856.0 eV, satellite: 861.6 eV, Ni $2p_{1/2}$:873.6 eV, satellite: 879.7 eV). The binding energy of the Ni 2p3/2 peak is difference from that in other reports of NiO (853.7 eV), NiS (853.1 eV) and Ni (852.6 eV),[3] but similar to the instances of $Ni(OH)_2$ (855.6 eV).[4]

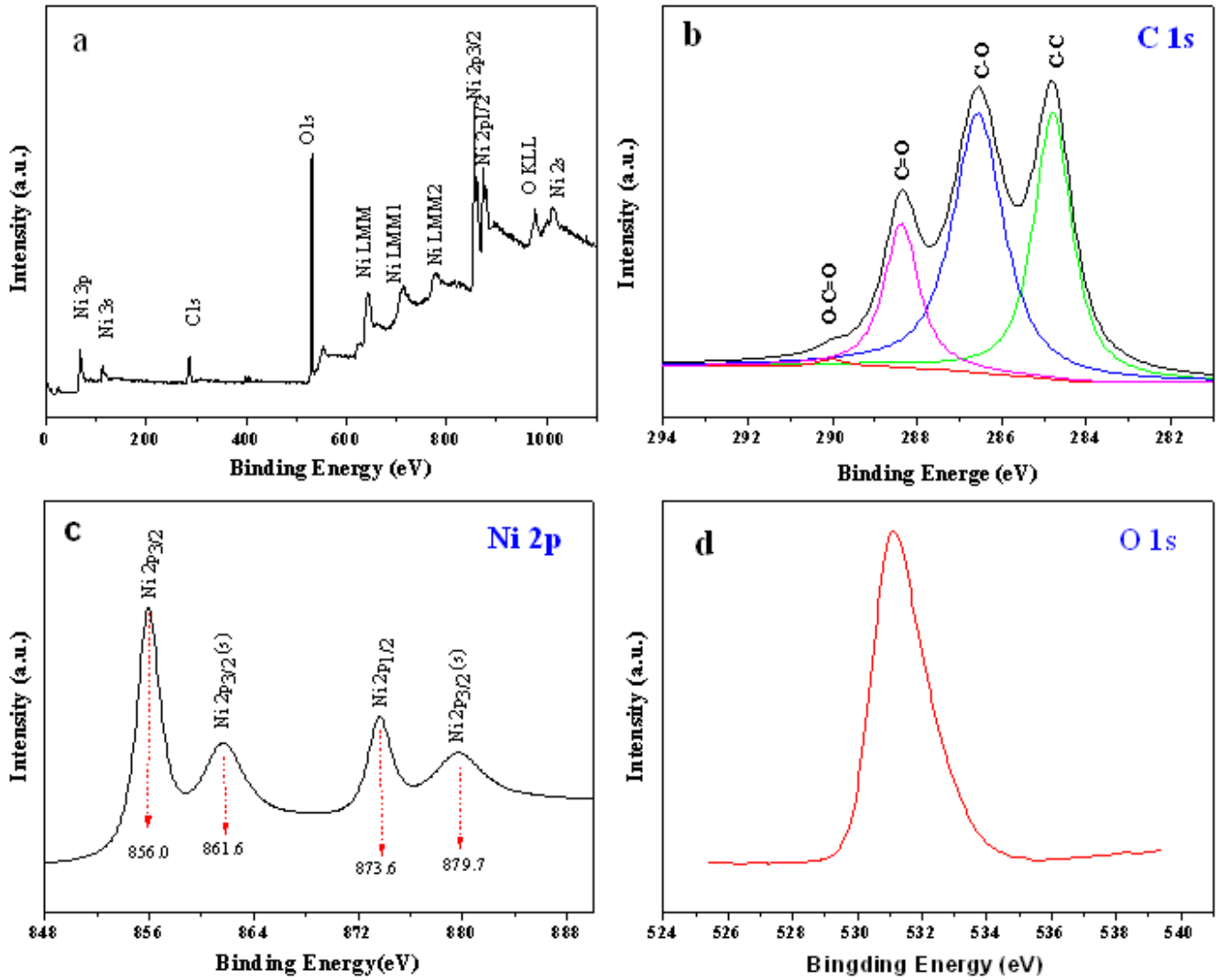

Fig. S3 XPS spectrum of GN20: (a) survey scan, (b) C 1s spectrum, (c) Ni 2p spectrum , and (d) O 1s spectrum.

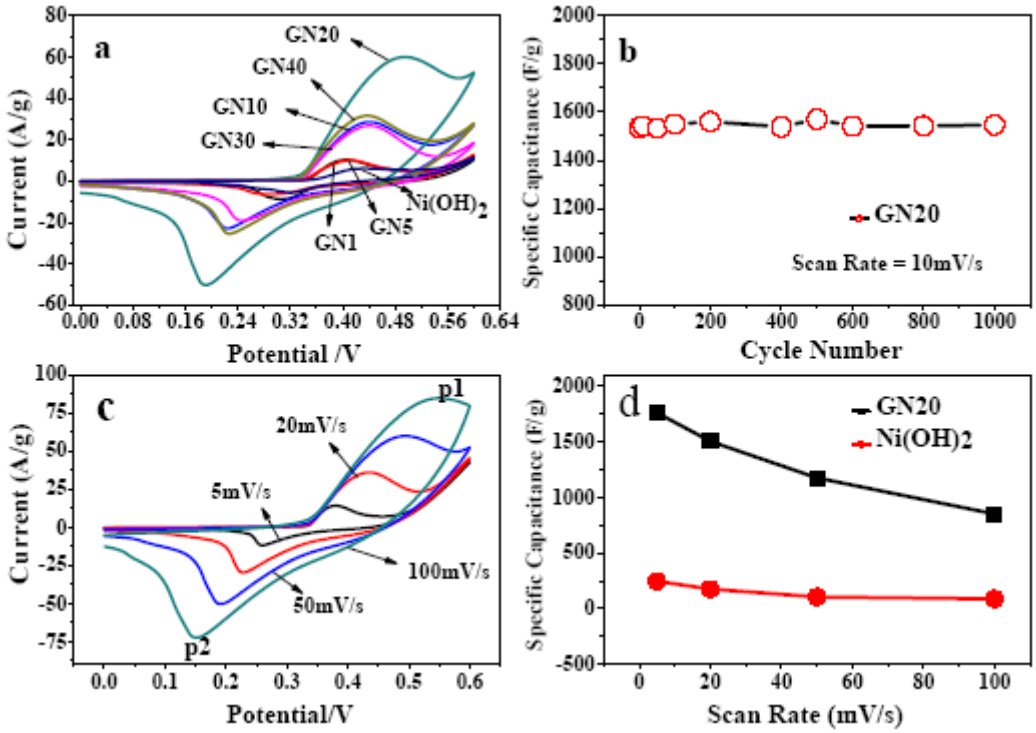

Fig. S4 Electrochemical characterization of graphene/α-Ni(OH)$_2$ composites and α-Ni(OH)$_2$. (a) CV curves of GN 1, GN 5, GN10, GN20, GN30, GN40, and α-Ni(OH)$_2$ at a 50 mV/s scan rate, (b) variation in the specific capacitance of GN20 as a function of the cycle number at a 10 mV/s scan rate, (c) CV curves of GN20 at various scan rates in 6.0 M KOH solution, and (d) specific capacitance of GN20 and α-Ni(OH)$_2$ as a function of the scan rate.

Table S1. Specific Capacitance Values of GN1, GN5, GN10, GN20, GN30, GN40, and α-Ni(OH)$_2$.

	5 mV/s	20 mV/s	50 mV/s	100 mV/s
GN1	228.04	190.28	165.70	149.45
GN5	217.58	182.64	160.77	144.86
GN10	752.20	615.01	512.08	423.38
GN20	1760.72	1504.28	1175.74	851.24
GN30	549.94	541.37	468.25	388.40
GN40	777.86	692.76	586.41	489.49
α-Ni(OH)$_2$	197.31	177.21	106.66	88.02

Specific capacitances (F/g) are calculated from CV curves.

N_2 adsorption-desorption studies were performed to determine the specific surface area of the GN composites and α-Ni(OH)$_2$. The summary of BET Surface area, pore size distribution and electrochemical properties of GN composites and α-Ni(OH)$_2$ were showed in Table S2. With increasing mass ratio, the BET area change, while the changes of average pore diameter take the same trend with the BET area. As the specific surface area of GO used is not high (48.95 m^2/g), the specific surface area of GN composites is also not high. The BET surface area of GN20 was found to be 63.582 m^2/g, which is the biggest one. The average pore diameter of GN composites was clearly larger than that of α-Ni(OH)$_2$. And it just accords with the conclusion of SEM ahead. The BET surface area of GN40 was found to be 54.34 m^2/g, which is not far from the area of GN20. However, the specific capacitance of GN40 is clearly smaller than that of GN20. This may be due to the distribution of pore diameter played a more important role in this case. The average pore diameter of GN30 was the largest one. We considered that the reason for this phenomenon is due to the pore size exceed an effective

range which do not partially contribute to the capacitance. It is clearly that the trend of decreasing BET Surface area trend is agreement with the capacitance values calculated from the CV curves. The change of the BET surface area is directly correlated to the specific capacitance.

Table S2: Summary of BET Surface Area and Electrochemical Properties of GN Composites and α-Ni(OH)$_2$.

	Specific capacitance (F/g)	Surface area (m^2/g)	Average pore size distribution (Å)
GN1	149.45	28.57	104.20
GN5	144.86	26.58	98.71
GN10	423.38	33.67	93.63
GN20	851.24	63.58	112.20
GN30	388.40	31.24	135.41
GN40	489.49	54.34	106.20
α-NiOH)$_2$	88.02	24.86	77.58
GO		48.95	147.89

Specific capacitances (F/g) are calculated from CV curves at a scan rate of 100 mV/s.

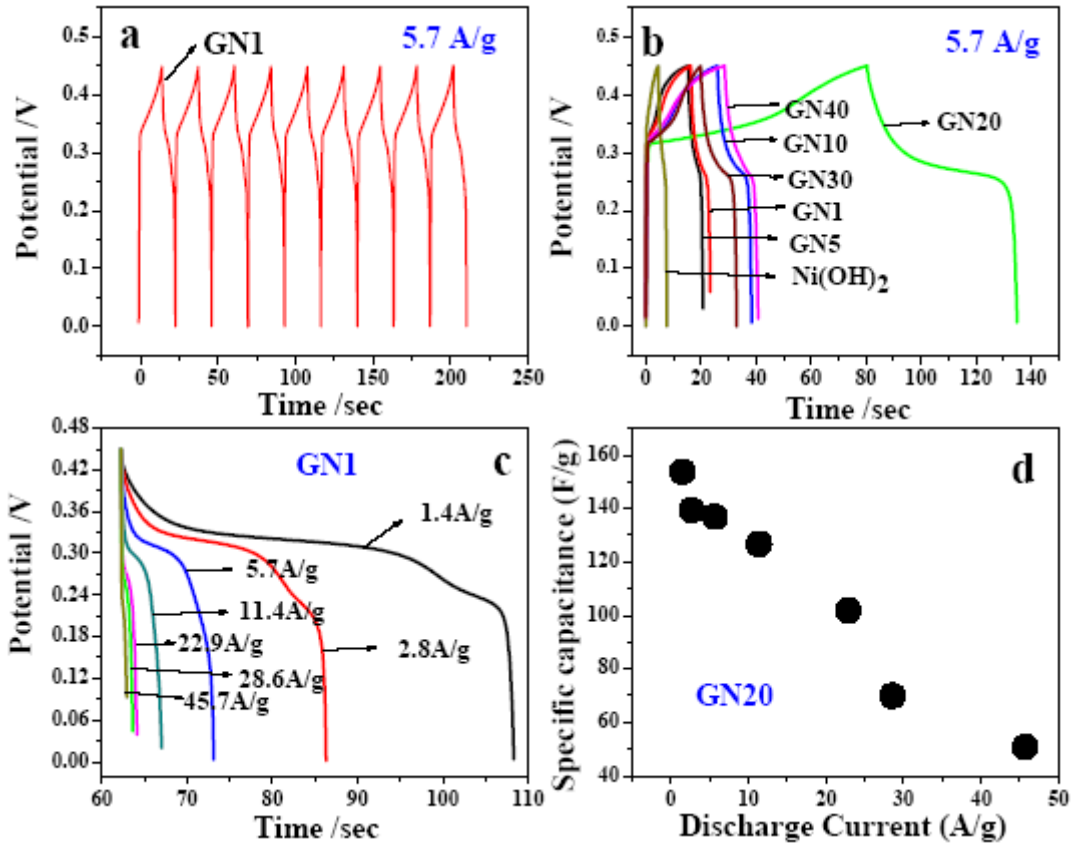

Fig. S5 (a) Galvanostatic charge and discharge curves of GN1 at a current density of 5.7 A/g. (b) Charge-discharge curves of graphite/α-Ni(OH)$_2$ composites and α-Ni(OH)$_2$ at a current density of 5.7 A/g. (c) Galvanostatic discharge curve of GN1 at various discharge current densities. (d) Average specific capacitance of GN20 at various discharge current densities.

Notes and references

1 H. L. Wang, J. T. Robinson, G. Diankov, and H. J. Dai, *J. Am. Chem. Soc.* 2010, **132**, 3270.

2 V. Chandra, J. Park, Y. Chun, J. W. Lee, I. C. H. Wang and K. S. Kim, *ACS Nano*, 2010, **4**, 3979.

3 V. Khomenko, E. Frackowiak and F. Beguin, *Electrochim. Acta,* 2005, **50**, 2499.

4 J. Liang, R. Ma, N. Iyi, Y. Ebina, K. Takada and T. Sasaki. *Chem. Mater.* 2010, **22**, 371.

5 G. Zan, W. Jun, Z. S. L and W. L. Yang, *Chem. Mater.* 2011, **23**, 3509.